Urban Climate 49 (2023) 101447

Contents lists available at ScienceDirect

Urban Climate

journal homepage: www.elsevier.com/locate/uclim

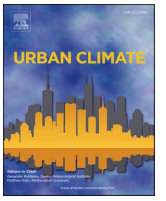

On kids' environmental wellbeing and their access to nature in urban heat islands: Hyperlocal microclimate analysis via surveys, modelling, and wearable sensing in urban playgrounds

Elena Tarpani [a], Ilaria Pigliautile [a,b], Anna Laura Pisello [a,b,c,*]

[a] CIRIAF - Interuniversity Research Center, University of Perugia, via G. Duranti 67, 06125 Perugia, Italy
[b] Department of Engineering, University of Perugia, via G. Duranti 63, 06125 Perugia, Italy
[c] The Department of Civil and Environmental Engineering, E209A Engineering Quadrangle Princeton, NJ 08544, USA

ARTICLE INFO

Keywords:
Urban Heat Island
Microclimate
Wearable device
children's thermal comfort
Outdoor comfort

ABSTRACT

The aim of this research is to investigate the environmental wellbeing of children in urban outdoor environments by developing and testing a new wearable device called the Baby c-air. Children are particularly vulnerable to environmental discomfort due to their physiological characteristics and lack of awareness about their own adaptation capabilities. This vulnerability can lead to childhood diseases and health issues, especially when exposed to overheating or continuous pollutants. Portable monitoring devices, such as the Baby c-air, can assess children's environmental exposure and provide timely information to limit their health risks.The study involved testing two prototypes of the Baby c-air under laboratory and in-field conditions to verify the accuracy of the device in collecting data. An experimental campaign involving 122 children was conducted in Italy during the summer, across four playgrounds. The option of integrating the COMFA-kid model for thermal comfort assessment was evaluated. The results indicated that microclimate peculiarities underline the importance of a human-centric approach for properly addressing environmental exposure. The discrepancies between thermal sensations provided by interviewed parents/tutors and predicted thermal sensations derived by the COMFA-kid model suggest that adults are generally weakly aware of children's thermal conditions.The Baby c-air can support children's adaptation potential and drive accompanying persons towards implementing conscious behaviors or moving to those areas with better environmental quality. The outcomes of this study can contribute towards urban outdoor design guidelines to improve children's well-being.

1. Introduction

Global climate change and urbanization are phenomena strictly correlated. Cities are responsible of 70% of the greenhouse gas (GHG) emissions and 2/3 of the energy consumption worldwide, directly affecting climate (Hoornweg et al., 2011). Moreover, cities forms and fabrics alter urban microclimate (Peng et al., 2022) and resilience to climate change (Kleerekoper et al., 2012) effects exposing the majority of global population, currently living in urban areas, to critical conditions.

Specifically focusing on thermally adverse scenarios, the combination of globally rising temperatures and the Urban Heat Island

* Corresponding author at: CIRIAF - Interuniversity Research Center, University of Perugia, via G. Duranti 67, 06125 Perugia, Italy.
E-mail address: anna.pisello@unipg.it (A.L. Pisello).

https://doi.org/10.1016/j.uclim.2023.101447
Received 12 August 2022; Received in revised form 28 November 2022; Accepted 11 February 2023
Available online 10 March 2023

phenomenon (Oke, 1982) has been demonstrated to generate hazardous conditions for people, increasing human mortality and causing adverse effects on human health (Campbell-Lendrum and Corvalán, 2007), (Zhao et al., 2011), (Laschewski and Jendritzky, 2002). Previous studies demonstrated that the individuals' thermal comfort perception and their psychological response are influenced by the configuration, materials for building skins (Castaldo et al., 2015; Fabiani et al., 2019), and the design of outdoor areas (Taleghani et al., 2015), (Middel et al., 2016) where the range of thermal "acceptability" is wider than indoor spaces (Nikolopoulou and Lykoudis, 2006), (Spagnolo and de Dear, 2003), (Thorsson et al., 2007). Urban Heat Island (UHI) intensification discourages people from spending time outdoors (Mazhar et al., 2015) and increase both mental health problems, such as eating disorders and depression (Chu et al., 2019), and physical health issues, such as cardiovascular disease and diabetes (Rodgers et al., 2018). Moreover, people who do not have the access to services considered essential for everyday life (e.g., heating, cooling, lighting) are inclined to spend time in the outdoor spaces and hence they are more exposed to local environmental boundaries and potential consequences on their health (Jessel et al., 2019). Among urban population, children represent a vulnerable category due to a lack in experience and capability of properly adapting to adverse conditions. In fact, recent studies have shown that children are more vulnerable to air pollution, extreme heat and radiation than adults (Vanos, 2015), (Balbus and Malina, 2009) and they are more exposed to the effects of climate change and more sensitive to high temperature than others. Air pollution causes several health issues, especially for the respiratory apparatus; a study conducted by Pènard-Morand et al. (Pénard-Morand et al., 2010) focused the attention on the asthma symptoms due to long-term exposure to outdoor pollution and demonstrated that the risk of suffering from asthma and other allergies is higher in children that live in the large cities. Other researches demonstrated the relationship between the high levels of pollution (due to the vehicular traffic, coal-fired power plants, etc.) and the decrease of lung function, the increase of sleep disordered breathing and the exacerbations of respiratory diseases in children (Bergstra et al., 2018), (Sánchez et al., 2019).

For these reasons, urban outdoors, and more specifically those areas designed to be attended mostly by vulnerable population like children, must be thermally comfortable and must have a low pollutants level (Kim et al., 2018), in order to increase their appeal among citizens, supporting their willing in doing physical activity and encouraging them to spend time outside. Indeed, Huang et al. (Huang et al., 2021) proposed design strategies to be adopted in playgrounds and parks for increasing outdoor children's comfort, using greenery and surface materials, such as high-near infrared paint and footprint pavement patterns; they established guidelines for architects and urban designers to create safe open spaces, able to mitigate urban heating and sun exposure. Moreover, Vanos et al. (Vanos et al., 2017) determined the large importance of vegetation and urban design in reducing heat and radiant exposures, especially when children were exercising in outdoors; they focused on bioclimatic design and calculated the children's energy budget during outdoor exercise, depicting the influence of both radiation and metabolism on children's heat balance and their thermal perceptions in outdoor recreational spaces.

These types of strategies lead to reduced health issues, in particular for children, who are more affected by extreme climate events due to climate change with respect to adults, but also less aware of specific adaptation actions (Teli et al., 2012). Moreover, studies have reported that children have physical and physiological differences compared to adults: they have higher surface area-to-mass ratio (Falk et al., 1991), (Tsuzuki-Hayakawa et al., 1995), lower body and immune system development (Watts et al., 2019), higher metabolic heat production (Brooks, 1948), lower sweat rate due to smaller sweat glands (Landing and Wells, 1969) and different ability to perceive the thermal environment (Mors et al., 2011). These fundamental differences influence the heat exchanges between children's bodies and the outdoor environment, which present different values compared to those calculated in adults. Nevertheless, most of the existing thermal comfort models (around 165 thermal indices for indoor and outdoor conditions identified in (Staiger et al., 2019)) account just for the adult's thermal sensation and preference and, thus, do not allow outdoor thermal comfort assessment for children.

Therefore, there is the necessity to properly adapt the energy balance between the human body and the environment considering the children's physical and physiological peculiarities for enhancing our prediction of their thermal comfort and preferences in outdoor spaces. An important study was conducted by Cheng and Brown (Cheng and Brown, 2020), which studied the COMFA model and modified some of its components (e.g., metabolic heat, convective heat and evaporative heat), taking into account the children's physical characteristics. The researchers released the COMFA-kid model as a result of an experimental campaign involving kids in the age range 7–12 years old.

Given this background, the present research work aims at investigating children environmental comfort in the urban environment (with a specific focus on kids under 5 years old) to provide insights on their resilience improvement. More specifically, such objective is here addressed by developing and testing a novel portable device which is proposed as reliable tool for the assessment of real kids' exposure to potentially harmful thermal and air quality conditions. The new monitoring system provides real-time evidence on kids' health risk in terms of both extreme heat and air pollutants exposure, in order to improve children's life quality and health and to prevent heat-related diseases and breathing pathologies over the years. Therefore, the study is composed in two main parts: (i) a prior validation phase of the prototypes' accuracy in data collection, that was carried out through both a laboratory and in-field test; and (ii) an experimental campaign designed to verify the appropriateness of including the COMFA-kid model in the same prototype as reference thermal model for the target group of the new tool (1-to-5 instead of 7-to-12 years old). The experimental campaign was conducted in four different playgrounds of Perugia, a middle-size Italian city. During the campaign, the main microclimate parameters were collected along with parents' evaluation of their kids' thermal comfort levels. Results of the questionnaire were thus compared to the predicted thermal comfort vote obtained from the COMFA-kid model (Cheng and Brown, 2020). Finally, the comparison of microclimate conditions observed in the four playgrounds pave the way for suggesting design guidelines of these outdoor spaces taking into account the environmental quality.

2. Materials and methods

The study aims at deepening kids' environmental comfort while developing and testing a new device addressing children's vulnerability to outdoor thermal stressors and air quality. Two prototypes were realized and calibrated both in the laboratory, under controlled thermal conditions, and in the field. Aside from prototypes calibration, the thermal comfort model COMFA-kid (developed for kids in the age range of 7–12) (Cheng and Brown, 2020) was tested for the thermal comfort assessment of kids in the age range from 1 to 5 to evaluate the appropriateness of including such model in the developed device. In this view, an experimental campaign was conducted in four outdoor spaces (e.g., urban parks and public playgrounds) located in the same city and characterized by different urban features (e.g., impervious surfaces, greenery, shading elements, etc.). The investigation took place during one week at the beginning of September 2021, in summer, and combined microclimate monitoring through a commercial compact weather station with the submission of a dedicated survey on kids' thermal comfort to be filled by their parents. Morphological differences of the selected areas further allowed assessment of their impact on the observed microclimatic conditions, as many studies have been provided (I. Lee et al., 2018), (H. Lee et al., 2013), (Schofield, 1985), (Rosso et al., 2022). The following subsections provide a detailed description of the innovative prototypes and the experimental procedures implemented during the different phases of the study (i.e., the calibration of the prototypes and the in-field experimental campaign) that are further summarized in Fig. 1.

2.1. The baby c-air device prototypes

The Baby c-air was conceived and designed as a portable device that continuously collects geo-referenced environmental parameters for the thermal and air quality assessment of the kids' surroundings. Technical specifics of the embedded sensors are detailed in Table 1.

The device looks like a children's toy, that can be worn, and arranged on the stroller or on a school backpack. The bottom part of the device, which embeds the sensing technology, was designed to allow external air flows and to avoid internal air stagnation while the upper part can light up in three different colours: it becomes green if the air quality and the thermal environment are good, yellow if they are moderate, and red if they are potentially unhealthy/hazardous. The system presents a rechargeable battery, and it can be associated with other devices via Bluetooth. A dedicated app shows the instantaneous values of the collected environmental parameters and allows to start a data recording session.

The above presented characteristics of the Baby c-air represent essential components of the new portable system which is currently patent pending. Given these characteristics, two prototypes of the Baby c-air were realized and tested in this work. These devices differ in terms of the design of their bottom part (openings on just one or two sides) and typology of embedded rechargeable battery (USB C or wireless).

The internal battery in both the prototypes last almost 3 h and all the data registered during their operation are locally saved into the internal memory of the connected smartphone. In the following, the prototype presenting a wireless rechargeable battery and openings just at its very bottom is named as BC1 (Fig. 2A), the other prototype BC2 (Fig. 2B).

2.2. Prototypes calibration

The Baby c-air accuracy in measuring the environmental parameters of interest was tested both under controlled thermal conditions and in the field.

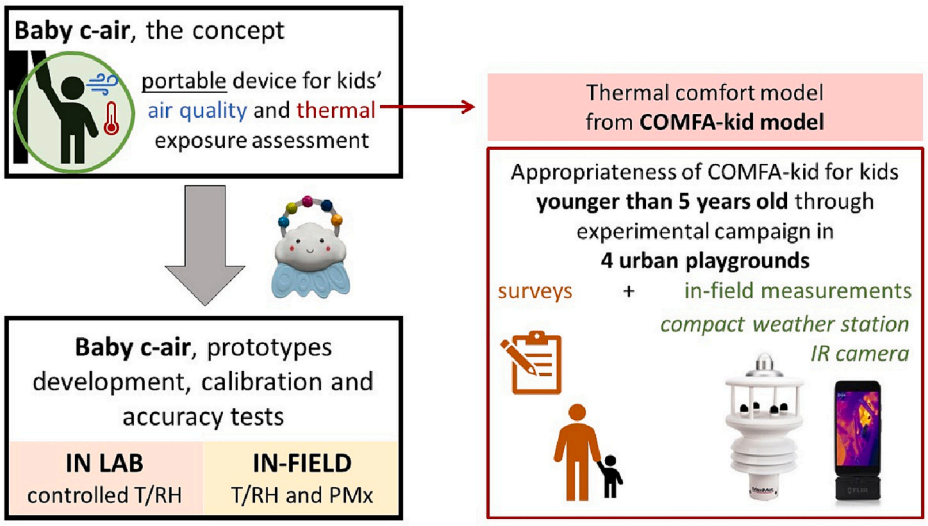

Fig. 1. Methodological framework of the study.

Table 1
Baby c-air embedded sensors specifics.

Monitored parameter	Sensor model	Technical specifics
Air temperature (Ta [°C])	BME280	Operation range: −40 °C–85 °C Absolute accuracy: ±1 °C at 0–65 °C
Relative humidity (RH [%])	BME280	Operation range: 10%–90% at 0–65 °C Absolute accuracy: ±3% at 20%–80% RH Response time: 1 s
Particulate matter concentrations (PM1.0, PM2.5, and PM10)	PMS5003	Effective range (PM2.5 standard): 0–500 μg/m^3 Resolution: 1 μg/m^3 Maximum consistency error (PM2.5 standard): ±10 μg/m^3 at 0–100 μg/m^3; ±10% at 100–500 μg/m^3 Total response time: <10 s

Fig. 2. The two prototypes (A) BC1 and (B) BC2, and (C) the interface of the app.

The laboratory test was performed in the climate chamber ATT DM 340 SR which allows to control the temperature and humidity condition of a 601 × 810 × 694 mm^3 test compartment in the range 233÷453 K.

The two prototypes were put in the climate chamber compartment, hung up to the internal metal grill along with two calibrated thermo-hygrometers (Tinytag Plus 2 – TGP-4500). The TGP-4500 models monitor temperatures from −25 °C to +85 °C, and relative humidity from 0 to 100% using built-in sensors (temperature accuracy ±0.5 °C; humidity accuracy ±3.0% at 25 °C). The climate chamber was programmed to replicate over a wide and representative range of conditions during four hours exposure: the settled temperatures ranged from 5 °C to 45 °C, with ramp of 5 °C raising temperature lasting 15 min every 10 min of temperature plateaus,

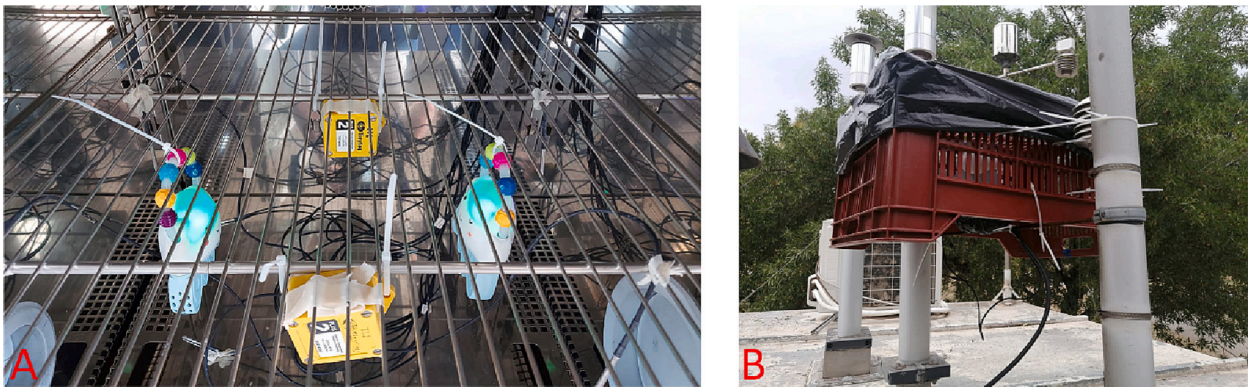

Fig. 3. (A) The two prototypes in the climate chamber and (B) the BC2 unit above the rooftop of the ARPA station.

while the range of relative humidity was from 70% to 20%, with decreasing ramp of 10% lasting 15 min, and the relative humidity plateaus of 10 min.

The in-field test consisted in installing one of the prototypes (BC2) in proximity of a station of the local environmental protection agency (ARPA) devoted to the collection of the pollutants concentrations in the urban background in combination with the main environmental parameters. More specifically, data retrieved by the ARPA station include: PM1.0, PM2.5 and PM10, wind direction and wind speed, air temperature, and relative humidity collected on an hourly basis. The BC2 unit was installed above the rooftop of the ARPA station for two weeks to retrieve a significant amount of data to be compared to the hourly values provided by the reference station. Despite the Baby c-air unit is not designed to be waterproof or to operate 24/7, the continuous operation of the device was guaranteed by directly connecting the BC2 to the power supply and associating the device to a smartphone acting as a gateway in the ARPA station for the whole monitoring. Furthermore, the device was protected by a pierced plastic box covered on its top with a black plastic membrane to guarantee shelter from precipitation that did not compromise the air flow. It is worth noting that, as in the laboratory configuration, the device was hung in the center of the plastic box to limit the influence of the black cover on the monitored air temperature. Nevertheless, possible affection of the designed shelter on gathered parameters is discussed in the results section. Fig. 3 shows (A) the assembly of the two prototypes in the climate chamber and (B) the position of the BC2 unit above the rooftop of the ARPA station.

2.3. Experimental campaign, kids' outdoor thermal comfort assessment

An in-field experimental campaign was conducted in summer 2021 to verify the applicability of the COMFA-kid model to kids in the age range from 1 to 5 years old (target of the Baby c-air). The experimental procedure involved the simultaneous collection of environmental boundaries through dedicated sensing apparatus and the kids' thermal perception via surveys specifically deployed for being proposed to their parents. The same procedure was replicated in four urban outdoors (specifically identified, as specified in Section 3), two times per day, from 10 am to 1 pm and from 4 pm to 7 pm. The same monitoring setup was replicated in each investigated outdoor space and the whole campaign was completed in one week.

2.3.1. Environmental monitoring

Environmental variables used as inputs for the children's energy budget were collected through a portable weather station (MaxiMet GMX501), settled at 1,80 m height from the ground, and gathering every second the following parameters: air temperature (accuracy +/− 0.3 °C), relative humidity (accuracy +/− 2%), pressure (0.1 hPa), solar radiation (spectral range 300 to 3000 nm), wind speed (accuracy +/− 3%) and wind direction (accuracy +/− 3°). Furthermore, infrared thermography, through the Flir One Pro thermal camera, was implemented to better characterize the radiative environment. The used IR camera captures images with solid thermal contrast, it has a thermal sensitivity of 70 mK and 160 × 120 (19,200 pixels) of thermal resolution. Infrared pictures were taken during each session at the beginning (almost 10 am in the morning and 4 pm in the afternoon), after 90 min, and at the end (almost 1 pm in the morning and 7 pm in the afternoon). Particular attention was given to the two main pavement finishes recognized in the area, as summarized in Table 3 for each playground. Finally, a reference fixed weather station was identified in the same city of the analysis (as detailed in section 3) to allow a comparison among microclimatic peculiarities of different selected playgrounds.

2.3.2. Survey

During the environmental monitoring campaign, surveys were distributed to those parents attending the investigated urban playgrounds with their children, if younger than 5 years old. The aim of the survey was to collect relevant information for computing children's energy budget according to the COMFA-kid model and for comparing the expressed thermal sensation with the predicted thermal sensation, therefore assessing parents' awareness about the thermal risk for their children. Indeed, even if the focus of the investigation were 1-to-5 years old kids, researchers directly interviewed their parents for a twofold aim: (i) 1–5 years old kids may not be capable of replying to our questions or have a limited perception of their-own comfort sensation; (ii) adults could provide their consent in taking part to an experimental campaign (as involved parents did at the beginning of the interview).

Therefore, the survey was made by 20 questions structured in three main sections: (i) general information, (ii) thermal perceptions and preferences, and (iii) routine and habits of the children. More specifically, retrieved general information include gender, age, height, weight, nationality, and for how long the child was living in the city of the experimental investigation. Additional general information were about the main activity performed by the child at the time of the interview and 15 min before, and the worn garments. The thermal perception of the surroundings was then deepened by asking for the thermal sensation, thermal comfort level and thermal preferences of the child through a 5-points scale. The same scale was further used to collect parents' opinion about their child perception of air humidity and wind, according to their experience and real-time observation. Finally, the parents had to provide the reason why they were coming to that specific outdoor space, from how long, and how often do they come to the same playground. The whole survey was framed in Google Form and submitted presented as QR code to the parents that could access the list of questions directly from their smartphones. Overall, 122 surveys were collected during the whole campaign.

2.3.3. Thermal comfort modelling

Retrieved environmental data and collected general information on the children attending the monitored area were used as inputs for the calculation of the children energy budget as presented by the COMFA-kid model. This is a modified version of the COMFA model (Brown and Gillespie, 1986), readapted by Cheng et al. for children in the age range from 7 to 12 years old (Cheng and Brown, 2020) accounting for their physiological differences compared to adults. Here, the focus of the analysis are young kids (younger than 5 years

old) and thus discrepancies observed between predicted thermal sensation through the COMFA-kid (PTS, associated to specific ranges of the energy budget, see Table 2) and collected actual thermal sensation votes (ATS) are analysed, while considering further differences in body physiology of young kids compared to COMFA-kid target (Cheng and Brown, 2020). Nevertheless, it is worth noting that all the changes implemented in the COMFA model for its adaptation to 7–12 years old kids are here included considering actual physical characteristics of the interviewed sample group (heigh and weight of the child).

The adopted formula for the preliminary assessment of children energy budget (EB) was the following.

$$EB = M + R_{abs} - TR_{emitted} - C - E \quad (1)$$

where M is the metabolic heat production, R_{abs} is the absorbed radiation, $TR_{emitted}$ is the re-emitted longwave radiation from the body towards the surroundings, C stands for the heat exchanged by convection, and E refers to evaporative heat exchanges. All the components are expressed in W/m^2.

The metabolic component of the budget depends on both (i) the resting metabolic rate (RMR, computed using the Schofield-WH equation (Schofield, 1985) that is valid for children until 10 years old) and (ii) the performed activity (Butte et al., 2018).

The absorbed radiative component, R_{abs}, accounts for (i) the incoming shortwave radiation and (ii) the long-wave radiation emitted by surroundings that are absorbed by the body. The shortwave component is computed as the radiation measured by the miniaturized weather station on-site reduced by the fraction reflected by the body, assuming a skin albedo to be 0.35 on average (Weyrich et al., 2006). The longwave component is simplified as made by the portion coming from the sky (depending on on-site monitored air temperature) and that coming from the ground (depending on ground surface temperature), equally weighted, thus assuming a view factor of 0.5 for both and no effects of vertical surfaces on the longwave radiation exchange with the body. The ground superficial temperature is derived by processing infrared shots taken during each experimental session accounting for different pavement typologies as specified in the description of the case study (Section 3).

The long-wave radiation emitted by the body, $TR_{emitted}$, relies on the calculation of temperature of the outer body layer that in the following is mentioned, for simplicity, as children skin temperature.

The heat loss due to convection, C, depends on the difference occurring between temperatures of the air, directly measured through the miniaturized weather station, and children core temperature that was computed considering the metabolic heat generated by a person; moreover, the other parameters considered for the computation of C are the heat flow resistances due to body tissue (r_t), clothing (r_c) and the air boundary layer around the body (r_a), as proposed in COMFA model (Cheng and Brown, 2020). The associated thermal loss was further corrected accounting for differences in body surface area (BSA [m^2]) and body mass (BM [kg]) between adults and children based on the Haycock et al.'s BSA equation (Haycock et al., 1978).

Finally, the evaporative heat exchange, E, was calculated as the sum of the evaporative heat losses occurring through perspiration and through the skin. According to the literature (Falk and Dotan, 2008), (Hugh et al., 2009), a child has approximately half the capacity to sweat than an adult, so the formula considered for the COMFA model was here modified considering half of the perspiration component.

Therefore, the thermal sensation vote for a kid in outdoors was established in the literature (Cheng and Brown, 2020) according to the computed energy budget as summarized in Table 2.

3. Case study

In this study, four playgrounds were selected as representative outdoor spaces for children's leisure activities. All the selected areas are situated in Perugia, central Italy, with humid subtropical climate (climate zone Cfa) according to the Köppen-Geiger classification (*World Maps of Köppen-Geiger Climate Classification*, 2023), (Kottek et al., 2006). The four playgrounds are, approximately, from 5 to 10 km apart. During the whole campaign, weather data were additionally collected by a fixed weather station located on the roof of the CIRIAF research institute, acting as a reference for the study. Fig. 4 shows a bird's eye view of the four playgrounds and the reference weather station location (indicated with the black point in the figure), while the Table 3 presents the main features of each playground and the percentage of the different types of identified surfaces. In detail, surfaces in playground A and B are divided into pervious (greenery, mainly lawn) and impervious (paths around the playground or the concrete basement of the playground gaming equipment). Pavements in playground C are divided in two different types of pervious coverage (lawn and cobblestone), Pavements in playground D are divided in two kinds of pervious surfaces (rubbery materials just below the playground and concrete tiles all around the installation).

Playground A (43°11′ N, 12°36′ E, 283,7 m above sea level) is the main urban park with an extension of 30.000 m^2. The selected

Table 2
Energy budget for the kid computed according to the COMFA-kid model and the corresponding Predicted Thermal Sensation (PTS).

Energy budget (EB) [W/m^2]		Predicted Thermal Sensation (PTS)
$EB \leq -140$	−2	Cold
$-140 < EB \leq -110$	−1	Cool
$-110 < EB \leq 40$	0	Neutral
$40 < EB \leq 80$	+1	Warm
> 80	+2	Hot

Fig. 4. Overview of the four playgrounds and the reference weather station and focus on each identified area where main surface types are identified such as the position of the monitoring system.

area presents different functions and services for people, and peculiarities aimed at creating a relaxing and enjoyable atmosphere for any users: coffee shop, playground area for infants and kids, paths, and fountains. The configuration of these playgrounds protects people from the chaos and the traffic of the city because the big parking and the main streets are in a decentralized position. During the monitoring campaign, the miniaturized weather station is arranged close to a bench near the centre of the park in order to record parameters similar to those perceived by children. Fig. 5. (A) illustrates the detail of the area where the urban park is situated. Playground B (43°11′ N, 12°44′ E, 209,2 m above the sea level) is a park mainly attended by residents of the same neighbourhood and thus referred, in the following, as a "residential park". Its extension is equal to 12.000 m^2 and it has a green path and several different attractions, such as the sporting area with two football fields and one basketball court. Playground C (43°08′ N, 12°44′ E, 198,5 m

Table 3
Characteristics of each playground.

Playground	Picture	Extension (m^2)	Type of surface (%)	Feature specifics
A		30.000	S1: 80 (lawn) S2: 20 (paths)	Presence of greenery, shielded areas and services, adjacency to the main streets and to the parking area
B		12.000	S1: 75 (lawn) S2: 25 (cement)	Presence of greenery and shielded areas, no specific services, adjacency to the residential and sporting area, presence of the parking area
C	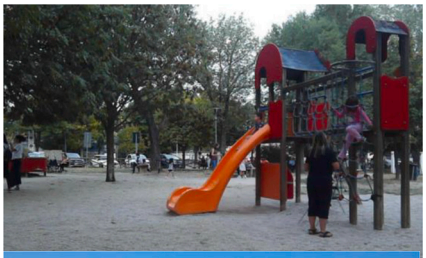	2.500	S1: 80 (cobblestone) S2: 20 (lawn)	Presence of a few greeneries, no specific services, adjacency to the residential zone, to the asphalt square and to the main streets, presence of the parking area
D		380	S1: 58 (rubbery materials) S2: 42 (concrete tiles)	Absence of greenery, presence of services, no shielded areas, adjacency to the commercial and sporting area, presence of the parking area

above the sea level), is a "residential park", mainly attended by the inhabitants of the neighbourhood but differing from the previous case since it is located near a generally congested vehicular arteria of the city and next to a big market square. The playground area (2.500 m^2) is surrounded by wide parking and an asphalted square. The area near the playground C is enclosed by main urban connections inside the neighbourhood. Finally, playground D is located near a shopping mall (43°09′ N, 12°31′ E, 252 m above sea

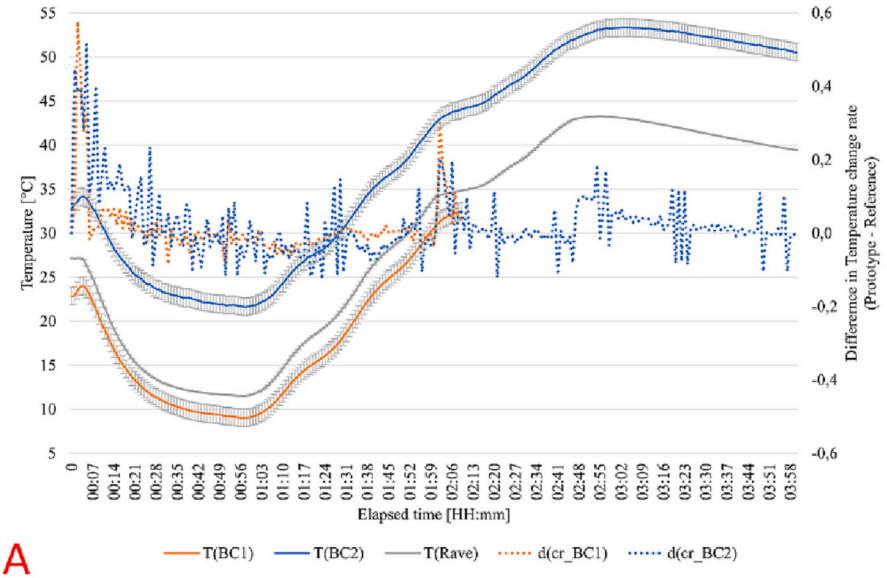

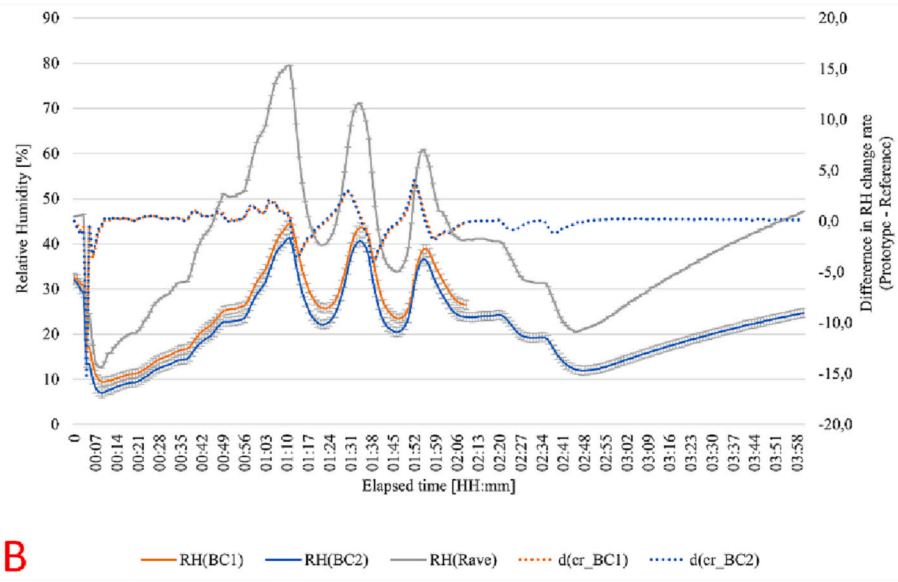

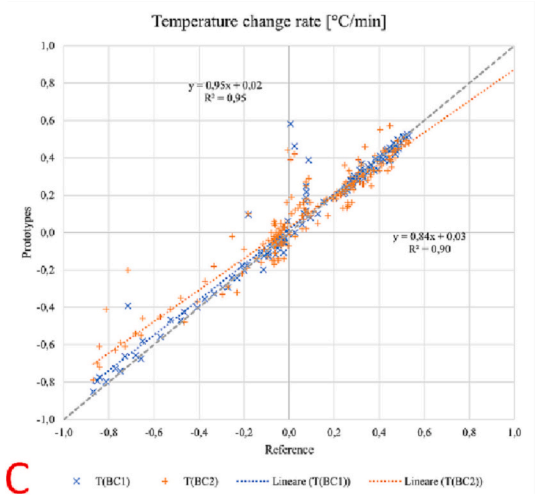

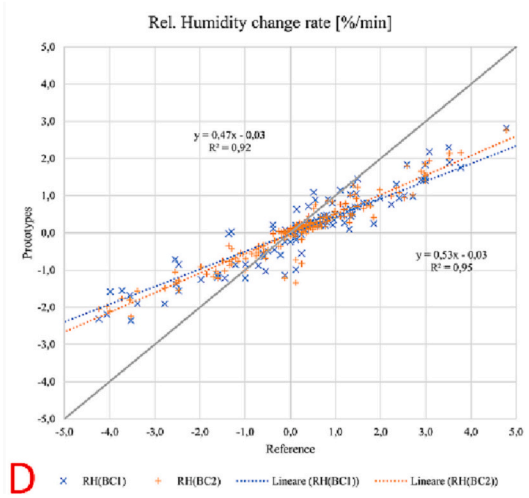

(caption on next page)

Fig. 5. Prototypes calibration through laboratory tests: (A) air temperature and (B) relative humidity trends in terms of absolute values and observed differences of the parameters rate of change with respect to the reference system; observed correlations between (C) air temperature and (D) relative humidity monitored by the prototypes and the reference.

level). It is smaller than the others, with an extension of only 380 m^2; there is no greenery, plants, or trees, and there are not several spaces where people can stay and relax. The only key playground elements are the benches on the perimeter of the playground. The playground is covered by a big structure (with a butterfly shape), built with steel and impervious materials, while the floor is designed with pervious coloured materials. The area where the playground D is located is enclosed by several streets and a large industrial area.

4. Results and discussions

4.1. Baby c-air calibration

4.1.1. Laboratory test

Graphs A and B of Fig. 5present the air temperature and relative humidity trends as monitored by the two prototypes and the two calibrated thermo-hygrometers. More specifically, values recorded by the two calibrated devices (S1 and S2) present differences that are smaller than the instrumental error (Bosch Sensortec, 2015) and thus just the average profile is reported. Data collected by the two prototypes present consistent trends for both air temperature and relative humidity demonstrating to have the same responsiveness to external stimuli. This is well-represented in graphs C and D of Figure 5, which relate air temperature and relative humidity change rate as registered by the prototypes and the reference system. The linear correlation is strong, presenting an R^2 coefficient always >0.9. Nevertheless, the thermohygrometer embedded in the Baby c-air prototypes is less responsive in humidity change detection presenting a linear correlation coefficient lower than the unit, i.e., equal to 0.47 and 0.53 for the BC1 and BC2 prototype respectively. These differences are comparable considering the two prototypes which means that the design of the element at the bottom of the Baby c-air is not affecting the quality of recorded environmental hygrothermal and air quality data. Considering the recorded absolute values, the BC2 unit registered higher air temperature values compared to the BC1 unit while both the prototypes recorded similar values for relative humidity (an average offset of 11 °C for air temperature, and of 2.7% for relative humidity). This huge discrepancy is a matter of compensation value to be used while programming the probe and it is not problematic at this stage of prototype development since it could be easily fixed.

4.1.2. In-field calibration test

The in-field calibration test is carried out to assess the accuracy of Baby c-air units in detecting both microclimatic parameters, i.e., air temperature and relative humidity, and pollutants concentration, i.e., PM2.5 and PM10. During the test, the temperature varies from a minimum of 13.7 °C up to a maximum of 36.7 °C while relative humidity varied in the range 32–86%, according with the reference ARPA station. Graphs in Fig. 6 present the microclimatic data measured with Baby c-air (BC2 unit) related to those retrieved by the reference sensors: in detail, (A) shows the air temperature values, while the (B) is referred to relative humidity data. Both graphs follow a straight trend, with a R^2 value of the liner correlation between data monitored by the BC2 prototype and the reference station equal to 0.93 and 0.95 for air temperature and relative humidity, respectively. This means that considering the correction factor to be used in the final sensor calibration procedure, the prototype captures actual variations of both ambient air temperature and humidity that are close to those observed by the reference system, even if slightly overestimating temperature and underestimating humidity. This over-estimation of air temperature is more evident for higher values suggesting a better data fit through a second-grade polynomial curve ($R^2 = 0.94$). This observation suggests that the prototype is sensitive to direct radiation and being under direct sunlight for a prolonged period could reduce the accuracy of temperature measurements. Moreover, it is possible that the black plastic membrane that was used to shelter the BC2 device (as shown in Fig. 3B) affected the microclimate just below the same membrane resulting in higher air temperature as actually observed by the prototype.

Fig. 7 presents the PM2.5 (A) and the PM10 (B) distribution recorded during the in-field calibration by the prototype and the ARPA station, respectively. In general, the PM2.5 values registered by Baby c-air look close to those measured by ARPA sensors: the mean concentration was 7.7 $\mu g/m^3$ and 7.4 $\mu g/m^3$, respectively. For PM10, the concentrations recorded by Baby c-air were lower than the values registered by the fixed station, but the mean concentration was similar: 18.1 $\mu g/m^3$ for Baby c-air, 17.6 $\mu g/m^3$ for ARPA.

In general, the percentage of error between the data measured through Baby c-air and the data recorded by the ARPA station was equal to 31% for PM2.5 and 38% for PM10. The correction of the percentage was adopted using the Root Mean Square Error (RMSE), a metric used to compare measured values through the prototypes (i.e., Baby c-air) with a reference data registered by the station (i.e., the station located on the top of the ARPA roof) (Sathishkumar et al., 2021). As well as for the air temperature data, it is worth noting that the sheltered box where the BC2 was placed may affect external air circulation possibly resulting in actually lower PMx exposure of the sensor despite the box design was conceived to guarantee free-floating of external air.

4.2. Experimental campaign

4.2.1. Urban playgrounds microclimate peculiarities

The experimental campaign was carried out for five days in summer 2021. Microclimatic parameters were gathered in each playground through the same miniaturized weather station during both a morning and an afternoon session, each lasting three hours.

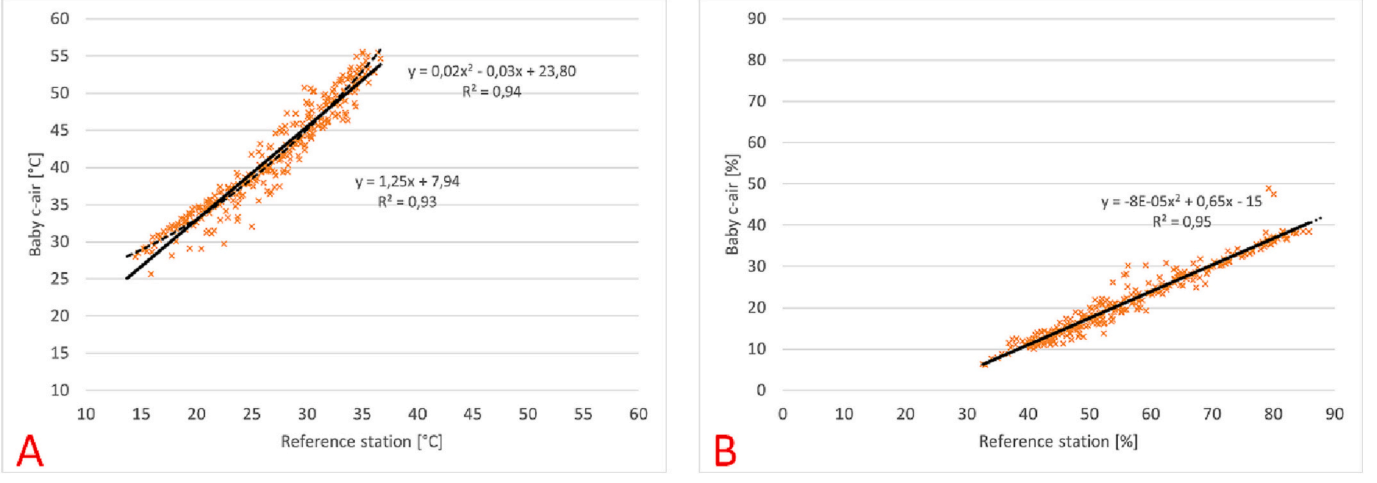

Fig. 6. Correlation of (A) air temperature and (B) relative humidity data collected by the Baby c-air and the reference station.

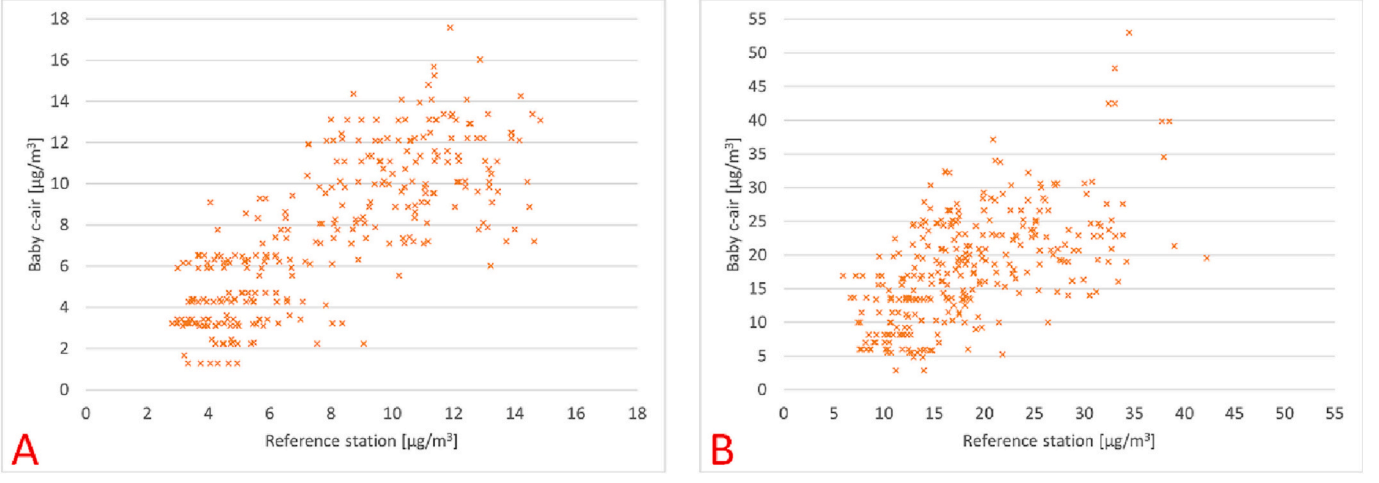

Fig. 7. (A) The PM2.5 and (B) the PM10 data recorded with Baby c-air and reference station.

Table 4
Data gathered during the morning and the afternoon campaigns from the compact weather station on-site and the reference one.

Playground	Time	T_a [°C] (ave)		RH [%] (ave)		WS [m/s] (ave)		SR [W/m^2] (ave)	
		Playground	Ref	Playground	Ref	Playground	Ref	Playground	Ref
A	10 am – 1 pm	25.4	25.6	42.0	31.0	1.51	3.18	756	895
	4 pm – 7 pm	27.0	25.9	43.0	39.0	0.80	2.37	11	160
B	10 am – 1 pm	24.4	26.0	53.0	36.0	0.77	1.68	248	768
	4 pm – 7 pm	27.2	26.0	39.0	30.0	0.60	1.55	31	192
C	10 am – 1 pm	23.9	24.1	50.0	40.0	0.81	1.75	651	818
	4 pm – 7 pm	27.9	25.3	39.0	39.0	0.76	1.96	39	84
D	10 am – 1 pm	26.2	25.9	42.0	33.0	1.22	2.75	665	831
	4 pm – 7 pm	28.6	24.9	31	30	1.30	3.94	313	199

Playgrounds were not monitored simultaneously and Table 4 summarizes the average values of air temperature, relative humidity, wind speed, and solar radiation gathered during each session by both the compact system on-site and the reference station. Air temperature data collected on-site, i.e., in each playground, were generally lower in the morning and higher in the afternoon compared to temperature values retrieved at the reference point. In fact, the on-site monitoring focuses on microclimatic conditions within the Urban Canopy (UC), inside the compact structure of the city, while the reference station is in an almost-open field. Therefore, sunrays enter the compact urban structure only once the sun reached the proper height on the horizon in the morning and the reduced Sky View Factor slows the cooling process in the afternoon. These temperature differences (i.e., playground compared to the reference) ranged between −0.2 °C and − 1.6 °C in the morning, observed at playground A/C and B, respectively, and + 1.1 and + 3.7 °C in the afternoon, observed at the playground A and D, respectively. Regarding the relative humidity, the average values retrieved at the four playgrounds were always higher than the data observed at the reference station with greater differences in the morning, i.e., discrepancies range of 9÷17%, with respect to the afternoon, i.e., discrepancies range of 1÷9%. On the other hand, wind speed data

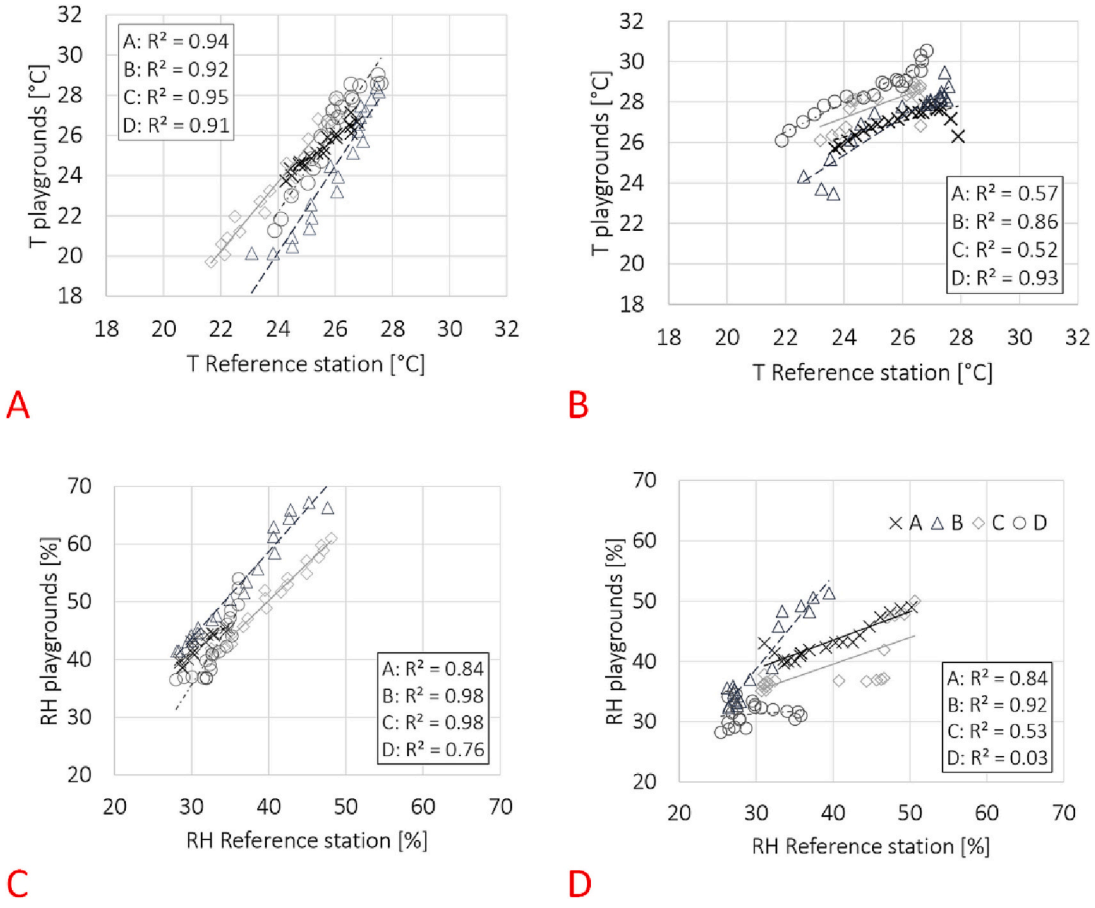

Fig. 8. Correlation between data retrieved on-site and at the reference station of air temperature (A, B) and relative humidity (C, D) during the morning (A, C) and in the afternoon sessions (B, D).

registered in the four playgrounds were always lower than those collected at the reference station, with an average difference of −1.43 m/s. As for the observed variation in the air temperature data, both relative humidity and wind speed conditions are representative of the internal position of the compact system used for the playground monitoring compared to the reference one. In fact, the reference station is located on a three-story building rooftop (an almost open-field location) while the four playgrounds are protected by buildings and trees that limit wind flow, while greenery, in general, could contribute to the air water vapor content through the evapotranspiration process. Finally, the average solar radiation presented in Table 4, for both the playgrounds and the reference point, suggests differences in terms of shadow availability among the four playgrounds. Furthermore, except for the case of playground D (the one in proximity of the commercial area and without greenery), average radiation values were between 11 and 39 W/m^2 in the afternoon suggesting that there was no availability of the direct shortwave component in those areas but only of the diffuse one. Observed reductions of the monitored solar radiation on-site compared to the reference one ranged between −16% and − 68% in the morning (at playground A and B, respectively) and − 53% and − 93% in the afternoon (at playground C and A, respectively). The higher average value for the solar radiation monitored in D with respect to the reference in the afternoon could be explained by the co-occurrences of two conditions: (i) the playground D is in a completely open area where incoming solar radiation varied from 596 W/m^2 down to 33 W/m^2 during the monitoring session; (ii) the reference station is in an almost-open area but faces a small hill on the South-West so that monitored radiation reached 0 W/m^2 almost 20 min before the end of the monitoring session.

These results could be imputed to the different configurations of the playgrounds: the amount of vegetation (and more generally of permeable surfaces) and the availability of big trees or other elements providing shadow represent an effective mitigation strategy to locally improve the outdoor microclimatic conditions for human comfort (Taleghani, 2018), (Ridha et al., 2018).

Graphs of Fig. 8 provide a direct comparison of each playground thermal profile by highlighting the correlation between air temperature (Fig. 8A and B) and relative humidity (Fig. 8C and D) data observed on-site and the data simultaneously retrieved at the reference station, for both the morning (Fig. 8A and C) and the afternoon sessions (Fig. 8B and D). More specifically, linear correlations and associated R^2 are presented. Air temperature data retrieved during the morning sessions are strongly correlated with temperature observations at the reference spot (R^2 >0.90) considering all the monitored playgrounds while in the afternoon similar results are shown just for playground D. Moreover, the linear correlation coefficients that are calculated for each thermal profile are always greater than one for the morning session and lower than one for the afternoon sessions. This outcome is in line with previous

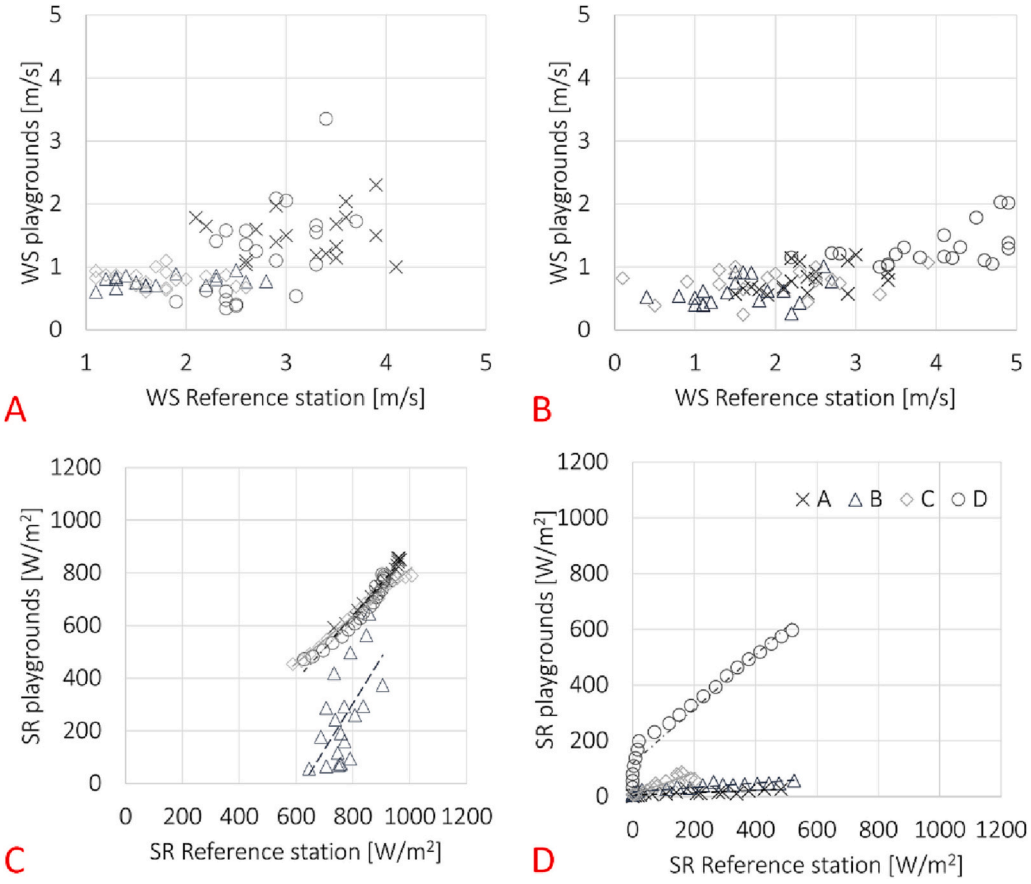

Fig. 9. Correlation between data retrieved on-site and at the reference station of wind speed (A, B) and solar radiation (C, D) during the morning (A, C) and in the afternoon sessions (B, D).

discussions since playgrounds' air temperature raised more rapidly from 10 am to 1 pm and decreased more slowly from 4 pm to 7 pm, than the reference spot. Focusing on relative differences among playgrounds, playground B always presents lower values of air temperature and higher levels of relative humidity which is imputable to its configuration with a large presence of greenery, that contributes to mitigate local microclimatic conditions. In the afternoon, playground D presented the highest temperature values (up to 29.5 °C) and the lowest relative humidity which was almost constant throughout the session (observed standard deviation of the retrieved data series equal to 1.8%).

Fig. 9 presents gathered on-site data against data collected at the reference station for wind speed (Fig. 9A and B) and solar radiation (Fig. 9C and D) registered during the morning (Fig. 9A and C) and afternoon sessions (Fig. 9B and D). Regarding wind speed data, as expected there is no correlation between wind speed values observed by the fixed reference weather station (which is in an open field, almost 10 m far from the terrain) and data collected at pedestrian level in each playground. Nevertheless, through the graphs it is possible to visualize and compare the windy conditions in each playground with respect to the weather boundaries of the specific monitoring day, as provided by the reference. The highest wind speed values were observed in playground D, up to 3.4 m/s and 2.0 m/s in the morning and afternoon sessions, respectively. Once more, the local microclimate peculiarities could be explained as resulting by the combination of the configuration of the area and the overall weather conditions. In fact, playground D was the most exposed to the open field air flow, while the others were protected by greenery and high trees, but at the same time that specific monitoring day was the windiest one according to data collected at the reference station.

Concerning solar radiation, the strong correlations of the morning sessions (R^2 above 0.90) show that both the playground and the reference station were under the same sky conditions. This is not the case only for playground B where solar radiation data in the morning are particularly scattered (standard deviation of 62 W/m^2 and $R^2 = 0.38$) most probably because of clouds passing by that area during the monitoring session. In the afternoon, playground D showed a significantly different profile compared to the others. As already mentioned, this is due to the openness of the are especially on its West side which caused almost 20 min of delay in the sunset.

Finally, the availability of incoming shortwave radiation coupled with specific fabrics of the investigated playground results in different warm up rates of the area in terms of superficial temperatures. These were characterized through thermographic inspection. Table 5 summarizes observed superficial temperatures throughout each monitoring session distinguishing between the two prevailing surfaces recognized in the area, i.e., S1 and S2 in Table 3, and providing the weighted mean superficial temperature for the area (T_{wa}) computed as the average of T_{S1} and T_{S2} accounting for the percentage in coverage of each specific type of surface as weighting factors.

The greatest variations observed throughout a single monitoring session were in playground D in the early morning and late afternoon, i.e., 0.12 °C/min and − 0.09 °C/min, respectively. These were mainly due to the variation of the rubbery pavement temperature (S1, covering 58% of the area) just below the playground equipment, probably installed for limiting kids' injuries. In playground C, the highest variation was observed in S1 temperature (cobblestone) from 11:30 am to 1:00 pm, from 24.0 °C up to 35.4 °C. Contrary, the greatest variation of superficial temperature in playground B was related to S2 (cement) in the late afternoon when a cooling rate of −0.07 °C was observed. Playground A showed minimum variations compared to the others with an overall difference in temperature of +3.9 °C and − 1.1 °C in the morning and afternoon session, respectively. Along with the focus on superficial temperature of the two most common finishes in each area, infrared pictures of the whole area were also taken to get an overview of temperature distribution. Figure 10presents an overview of superficial temperature spatial variations in playground D

Table 5
Superficial temperature of the two pavements mainly characterizing each playground (T_{S1} and T_{S2}) and resulting weighted average (T_{wa}) throughout the monitoring sessions.

Playground	Time	T_{S1} [°C]	T_{S2} [°C]	T_{wa} [°C]
A	10:00 am	21.3	22.0	21.4
	11:30 am	22.0	25.1	22.6
	1:00 pm	24.1	30.2	25.3
	4:00 pm	23.3	24.6	23.6
	5:30 pm	22.0	23.5	22.3
	7:00 pm	22.3	23.1	22.5
B	10:00 am	19.0	24.2	20.3
	11:30 am	23.6	25.0	24.0
	1:00 pm	24.4	26.4	24.9
	4:00 pm	25.6	33.6	27.6
	5:30 pm	25.2	27.8	25.9
	7:00 pm	21.0	21.8	21.2
C	10:00 am	19.7	24.2	20.6
	11:30 am	24.0	26.2	24.4
	1:00 pm	35.4	31.4	34.6
	4:00 pm	24.2	27.3	24.8
	5:30 pm	23.9	25.6	24.2
	7:00 pm	22.4	25.3	23.0
D	10:00 am	18.3	22.7	20.1
	11:30 am	31.0	31.5	31.2
	1:00 pm	37.9	33.3	36.0
	4:00 pm	33.9	35.2	34.4
	5:30 pm	31.8	34.4	32.9
	7:00 pm	23.0	28.2	25.1

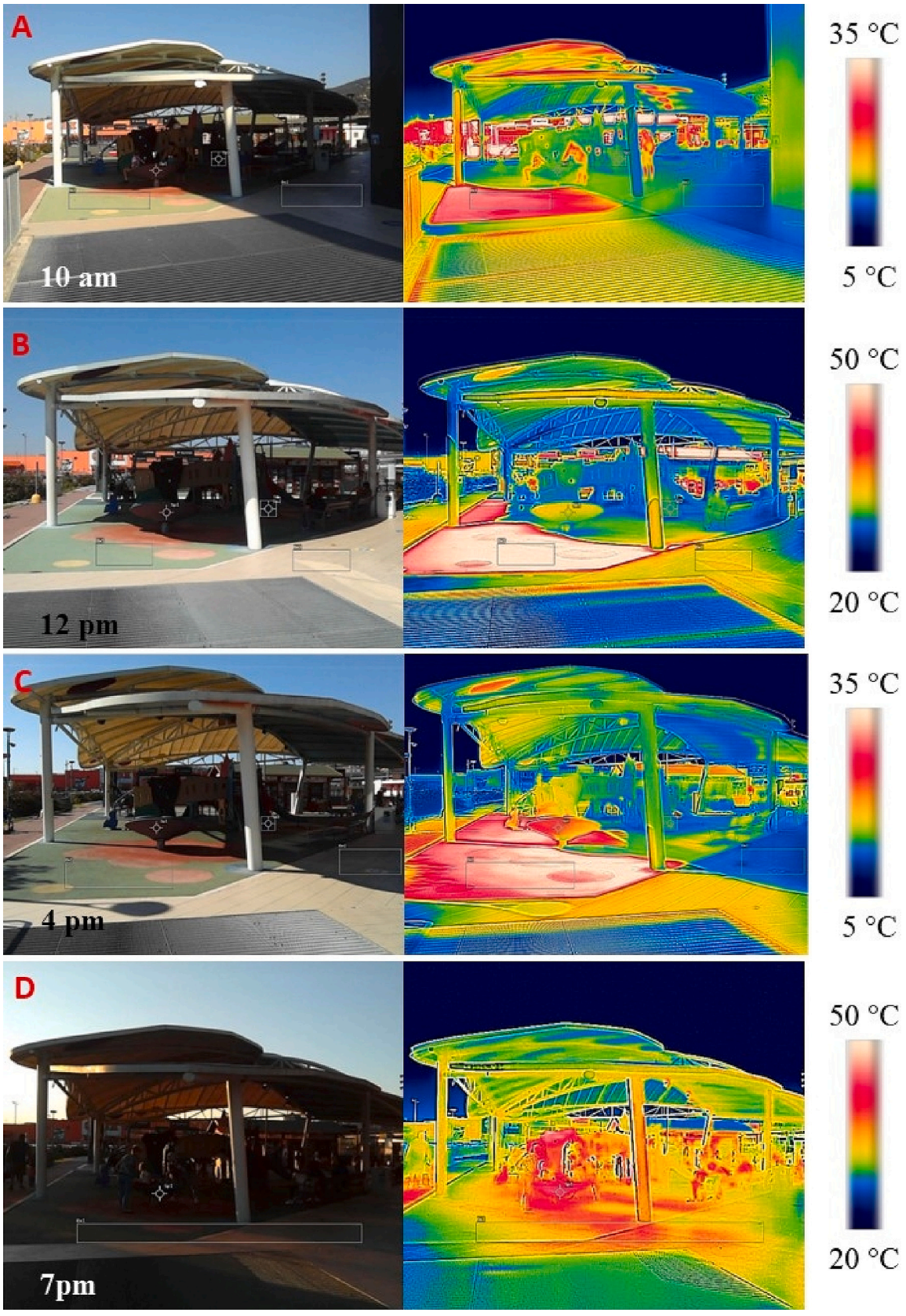

(caption on next page)

Fig. 10. Thermographic inspection at playground D, shots taken at the beginning and in the end of each monitoring session: (A) 10 am, (B) 12 pm, (C) 4 pm, and (D) 7 pm.

throughout the monitoring sessions. Except for the late afternoon (Fig. 10D) the portion of rubbery finishes not sheltered was always much warmer than the rest.

4.2.2. Kids' thermal comfort assessment

A total of 122 children were involved in the campaign by directly interviewing their parents. Overall, the interviewed sample was made by 70 girls and 52 boys, between 1 and 5 years old (mean 3.2 years old for girls and mean 3.1 years old for boys). Table 6 shows the distribution of the subjects in the four playgrounds, considering the date and the time of the campaign. The minimum number of interviewed per session was 12 (during both the monitoring at playground C in the morning and at playground D in the afternoon) and the maximum 20 (at playground A in the afternoon).

Table 7 presents the mean, median, and standard deviation of the children's energy budget calculated by the COMFA-kid model (as presented in the section 2.3.3) considering data retrieved in each session. The highest values of the mean energy budget were registered in playground D both in the morning and the afternoon sessions, with a value equal to 347.53 W/m^2 and 323.14 W/m^2, respectively. On the other hand, the lowest mean energy budget values were observed in playground C, with 72.78 W/m^2 and 95.85 W/m^2 for the morning and the afternoon session, respectively. Overall, the mean EB value was 243.94 W/m^2 and 155.53 W/m^2 for the morning and the afternoon, respectively; the median and the SD were 357.31 W/m^2 and 190.39 W/m^2 for the morning, while 46.25 W/m^2 and 150.02 W/m^2 for the afternoon, respectively.

Fig. 11provides an overview of the Energy Budget computed for each kid whose parents were involved in the experimental campaigns. Graphs show the contribution of each budget component: those providing a heat gain for the body (i.e., M and R_{abs}) and those representing heat losses (i.e., $TR_{emitted}$, C, and E). During the central and hottest hours of the day, i.e., late morning and early afternoon, playground D was characterized by the highest values in terms of kid's energy budget, exceeding 400 W/m^2. Peculiarities of playground D, forms, fabrics, and functions of the area (its openness, the absence of permeable surfaces, and the proximity to a commercial hub) resulted in a not thermally comfortable microclimate for children, especially around noon: the materials tend to significantly warm up throughout the day, as confirmed by the analysis of the thermal images realized during the campaign. Becoming a primary source of heat, the playground surfaces vanish the contribution of existing shelters in limiting local overheating phenomena or in providing thermally comfortable conditions. The two paddle fields (cement surfaces), located next to the park, further contribute to the growth of temperature. Furthermore, graphs of Figure 11 clearly highlight the role of greenery and, more specifically, of shadow availability in the area since the absorbed radiation (accounting for both shortwave and longwave components) was the most fluctuating component of the energy budget being the primary cause of uncomfortable thermal conditions, i.e., above 80 W/m^2. This outcome could limit the accuracy in children thermal risks prediction of devices such as the here presented Baby c-air do not monitor the radiative environment, because of major cost of the reliable equipment and the idea of providing the large urban public with this prototyped sensor. Therefore, it would be of utmost importance the integration of multiple monitoring systems and different levels of information. For example, the risks accuracy of a portable and personalized system could be enhanced by the possibility to communicate with fix weather stations and to access GIS data: from fix weather stations data about radiation and wind field could be retrieved and integrated, while GIS data would provide relevant information on the area characteristics that could further detail the expected local microclimatic conditions supported by real-time monitored data from the portable device.

The computed energy budgets provide the children predicted thermal sensation vote (PTS) according to the model defined by Cheng et al.(Cheng and Brown, 2020). Here, the energy budget resulting from the COMFA-kid model adoption is associated to the corresponding PTS whose ranges are summarized in Table 2. These predicted thermal sensations are compared with the actual thermal sensation votes (ATS) as expressed by children's parents (adults interpreting children sensations) via survey through the proposed 5-points scale: ranging from −2 (the child is feeling cold) to +2 (the child is feeling hot) where 0 means thermal neutrality. Fig. 12 presents the frequency distribution of the occurring gaps between the PTSs computed according to monitored environmental parameters and kid specifics attributes (i.e., gender, BMI, performed activity, and clothes) and ATS votes collected via surveys in all the four playgrounds, separately.

Table 6
Distribution of the subjects in each playground.

Playground	Time	Number of subjects		Age (ave ± sd) [years old]
		Male	Female	
A	10 am – 1 pm	6	9	2.7 ± 0.9
	4 pm – 7 pm	8	12	3.2 ± 1.3
B	10 am – 1 pm	7	8	2.5 ± 1.2
	4 pm – 7 pm	10	7	2.6 ± 1.1
C	10 am – 1 pm	6	6	3.8 ± 1.1
	4 pm – 7 pm	6	9	3.2 ± 1.4
D	10 am – 1 pm	6	10	3.3 ± 1.2
	4 pm – 7 pm	3	9	3.8 ± 1.1
	Total	52	70	3.1 ± 1.2

Table 7
Children's energy budget from COMFA-kid model: mean, median, and standard deviation (SD) for each session.

Playground	Mean EB (W/m^2)		Median (W/m^2)		SD (W/m^2)	
	Morning	Afternoon	Morning	Afternoon	Morning	Afternoon
A	290.96	133.50	368.60	10.00	169.86	189.81
B	232.85	92.72	346.03	36.85	227.56	114.60
C	104.40	72.78	75.59	55.66	130.85	95.85
D	347.53	323.14	378.67	456.11	233.28	200.34
Total	243.94	155.53	357.31	46.25	190.39	150.02

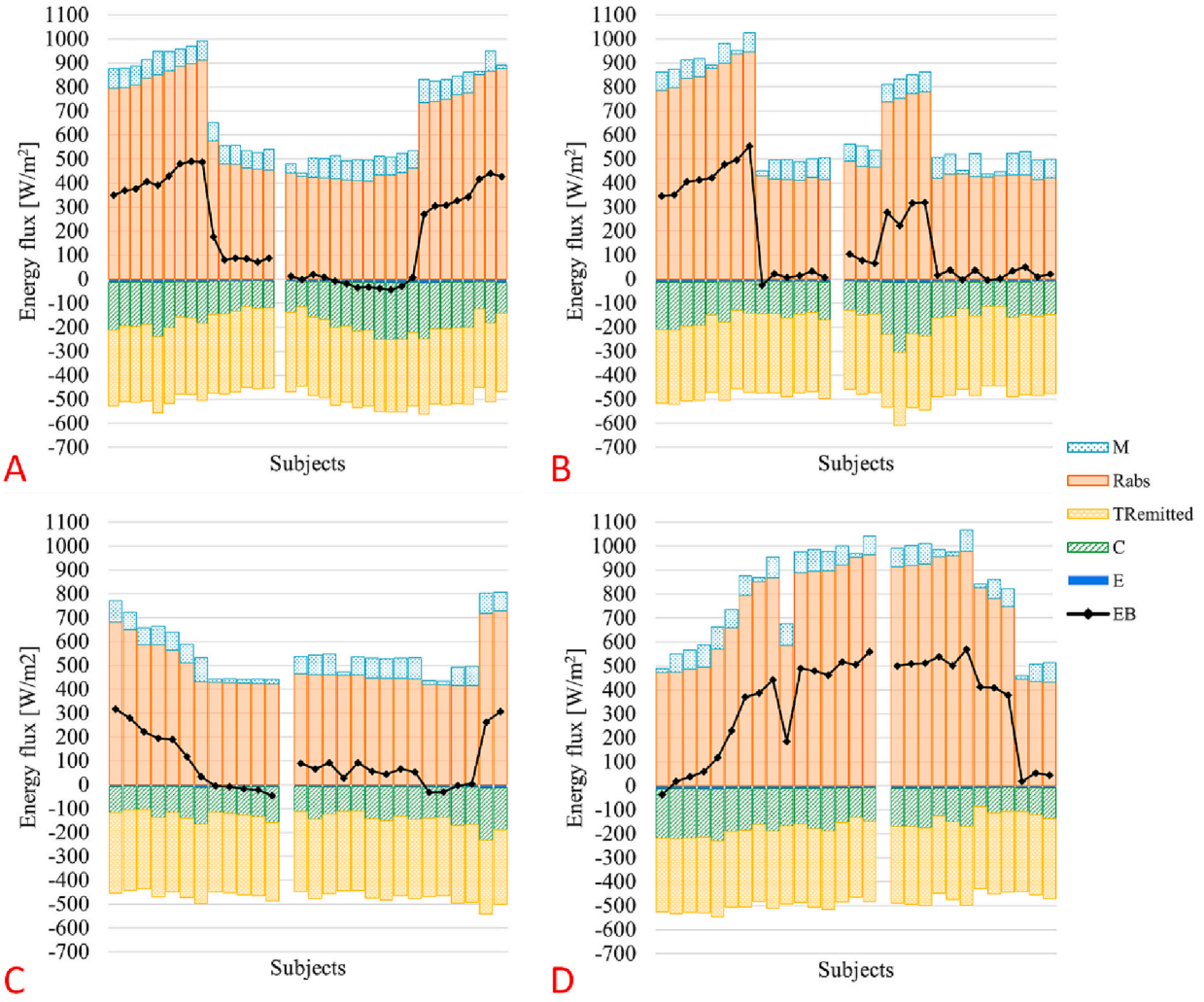

Fig. 11. Detailed Energy Budget of all the kids whose parents were interviewed during the experimental campaign at each playground.

The comfort model, and thus the PTS, seems to predict quite well the expressed thermal sensation for the two case studies of playground B and C where most of the PTS correspond to the ATS resulting in a difference of zero, i.e., 34% and 52% of votes for B and C, respectively. On the other hand, PTS are one point greater than ATS for most of the retrieved surveys in playground D, i.e., 43% of votes. This observed gap is even larger in playground A where PTS votes are generally two points greater than ATS retrieved by surveys, i.e., 34% of the cases. These differences could mean that the COMFA-kid model overestimates (PTS-ATS > 0) the actual sensation or that parents underestimate their children's sensation maybe relying upon their own sensation. According to literature, the letter hypothesis seems the most plausible one. In fact, the same study presenting the COMFA-kid model and its validation (Cheng and Brown, 2020) highlighted that children in the age range of 7–12 years old are more sensitive to warm and hot conditions compared to adults, also because of a sensibly higher metabolic rate. Similar considerations could be extended to younger children (below 5 years old) that are the main target of the present research and that should be even more sensitive than the 7–12 years old kids to thermal stress.

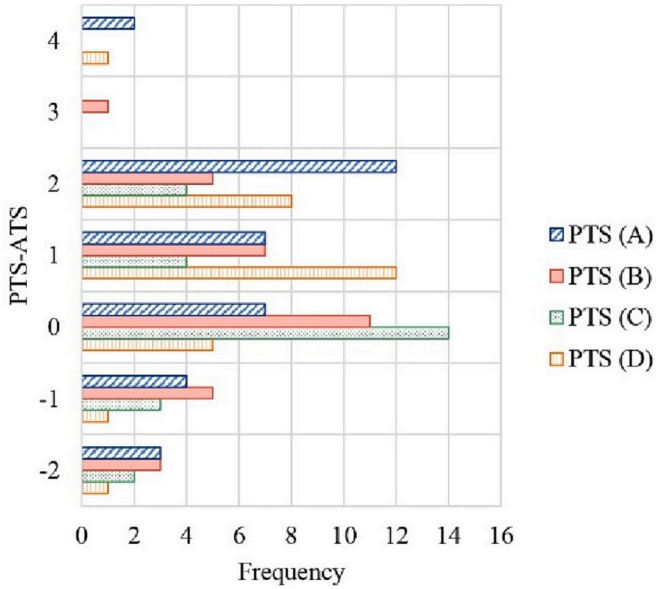

Fig. 12. Frequency distribution of the occurring difference between PTS and ATS for each playground.

Moreover, differences observed among playgrounds suggest that the parents' capability of addressing their children's thermal sensation could be compromised by the appearance of surroundings. As a matter of fact, this happened in the two playgrounds that are not close to residential areas (so you need to reach them on purpose): the urban park (playground A) and the playground at the commercial hub (playground D). In the latter case, this could be particularly dangerous for the safety of the child since there the worst thermal conditions were experienced, as specified in the analysis of Fig. 12.

5. Conclusions

Children's physical and physiological differences compared to adults contribute to their different thermal regulations and thermal responses in the various outdoor spaces. Children have higher metabolism and lower sweating rate compared to adults, that causes less evaporative heat exchange with the environment. Therefore, children are more sensitive to warm and hot conditions compared to adults but are less capable of adapting to the surroundings to achieve their thermal neutrality. Moreover, children are more vulnerable to pollutants exposure which is another physical threat to their health coming from the environment. For this reason, it is fundamental to carefully address children thermal and air quality risks by combining proper tools for assessing their exposure to environmental boundaries which relies upon tailored comfort models (accounting for their vulnerabilities) to process collected environmental information in real-time and to provide alerts on the environmental risks children are exposed to. In order to do so, the development of miniaturized and potentially simple and low-cost monitoring systems offers promising opportunities.

This work presents a newly developed wearable and portable device for children environmental risk assessment, the Baby c-air, which is able to monitor microclimatic and air quality conditions. Along with the prototype design and calibration, the study focuses on the application of the COMFA-kid model for children's thermal comfort assessment in four different playgrounds that were identified for their differences in form, fabrics, and surrounding urban functions.

Baby c-air calibration procedure involved both an in-lab and an in-field test providing the operational range and accuracy of the system. During both the procedures, the two prototypes demonstrated to be reliable in monitoring both thermal and air quality parameters, presenting the same responsiveness to external stimuli of the reference systems with no significant differences for the two prototypes: the design of the bottom component of the Baby c-air seems to not affect its accuracy in data gathering. Nevertheless, Baby c-air is sensitive to direct radiation and prolonged exposure to direct sunlight could reduce its temperature measurements accuracy. An improvement of the Baby c-air could consist in the integration of a radiation shield for the embedded thermo-hygrometer.

Regarding the microclimatic conditions of the four playgrounds, results show that the different configuration and location of the playground massively affect local environmental conditions, such as air temperature, relative humidity, wind speed, and solar radiation having a potential detrimental role in kids' comfort and vulnerability to local overheating in summer. Playground D, the only one that does not provide any shaded spaces and has no greenery, presented the highest temperatures (up to 28 °C during the afternoon sessions, 1.4 °C higher on average that the other studied playgrounds) and the most critical thermal conditions for the children. Moreover, this playground is in an open field condition, without any obstacles that can limit the air flow and the incoming solar radiation; hence, the exposition to the solar radiation is higher compared to the others, which present a wider amount of vegetation and greenery, and thus shaded spaces. Here, the computed energy budget of the kids reaches a maximum of 570 W/m^2, far beyond the threshold of predicted hot thermal sensation, i.e., 80 W/m^2. The observed microclimate peculiarities at local and hyperlocal scale

suggests once more the importance of implementing human-centred investigation to properly assess real exposure of individuals to environmental boundaries. At the same time, portable devices cannot monitor a complete set of weather parameters. For example, it is rare that a miniaturized portable system could properly detect the radiative environment and thus the integration of portable system, such as the Baby c-air, with fix and more sophisticated ones should be pursued in the development of such technologies.

The comparison between actual thermal sensation votes, retrieved via surveys, and predicted thermal sensation votes, computed according to ranges provided by the COMFA-model, provided insights on possibly biased judgment of children thermal status from their parents (adults). A minimum accordance between ATS and PTS was verified for the playground D, i.e., 18% of provided answers. This outcome further underlines the importance of developing tools capable of providing tailored alerts for reducing the environmental risks for children by accounting for their physiological peculiarities.

Finally, this study supports, through a specific and quantitative approach, the evidence that the design, and the specific location/context of a playground (and in general of the children's outdoor spaces) represent strategic elements in urban planning, since these influence children's outdoor comfort and well-being. Indeed, the analysis of the selected playgrounds microclimate peculiarities showed that vegetation and permeable surfaces guarantee mitigated microclimatic conditions by improving children's outdoor thermal comfort. Similarly, the presence of trees further impacts the local microclimate by shading direct solar radiation and limiting the air velocity in the area. These outcomes specifically refer to summer boundary conditions (the season presenting extreme weather conditions and a higher attendance rate) but highlighted differences in terms of form, fabrics, and surroundings urban functions are expected to generate slightly different local microclimatic conditions also in winter. As a future step of the research, the repetition of the same experimental campaign in winter will provide the experimental basis for a year-long assessment of urban playgrounds environmental quality.

It is therefore essential for architects and designers to consider proper shading and any mitigation strategies (e.g., greenery, pervious surfaces, cool materials, etc.) in order to improve the microclimatic condition for both adults and children. It is even more important to plan the outdoor spaces considering the children's requirements and needs in those neighborhoods largely affected by energy poverty since playgrounds at public parks may be children's only regular access to nature. Local outdoor restoring areas may address a fundamental social community role of aggregation, while potentially increase sensitivity and exposure risks to the weakest groups of population, i.e. children, elderly people, and energy poor ones.

CRediT authorship contribution statement

Elena Tarpani: Methodology, Software, Validation, Formal analysis, Investigation, Data curation, Writing – original draft, Visualization. **Ilaria Pigliautile:** Conceptualization, Methodology, Validation, Investigation, Data curation, Writing – original draft, Visualization. **Anna Laura Pisello:** Conceptualization, Methodology, Validation, Investigation, Resources, Writing – review & editing, Supervision, Project administration, Funding acquisition.

Declaration of Competing Interest

The authors declare that they have no known competing financial interests or personal relationships that could have appeared to influence the work reported in this paper.

Data availability

Data will be made available on request.

Acknowledgments

Authors from University of Perugia wish to thank the European Union's Horizon 2020 program under grant agreement no. 890345 (NRG2peers) for supporting their research. Elena Tarpani acknowledgments are due to the PhD School in Energy and Sustainable Development from University of Perugia (Italy). Ilaria Pigliautile and Elena Tarpani would like to thank the Italian funding program *Fondo Sociale Europeo REACT EU – Programma Operativo Nazionale Ricerca e Innovazione 2014-2020* (D.M. n.1062 del 10 agosto 2021) for supporting their research through projects "*Red-To-Green*" and "*Comunità Energetiche Resilienti per la valorizzazione del benessere ambientale, del risparmio energetico e della valorizzazione del patrimonio mediante gestione multidominio di dati "Human Centric*", respectively. The authors also thank EAPLAB members at CIRIAF (University of Perugia) - www.eaplab.net, for contributing to the massive field tests together with the students of Building Engineering class at University of Perugia. Additionally, the authors specifically thank dr. Benedetta Pioppi for supporting this idea and the technology uptake of Baby c-air.

References

Balbus, John M., Malina, Catherine, 2009. Identifying vulnerable subpopulations for climate change health effects in the United States. J. Occup. Environ. Med. 51 (1), 33–37.

Bergstra, Arnold D., Brunekreef, Bert, Burdorf, Alex, 2018. The effect of industry-related air pollution on lung function and respiratory symptoms in school children. Environmental Health: A Global Access Science Source 17 (1), 1–9.

Brooks, C., 1948. The regulation of body temperature. Med. J. Aust. 1 (8), 221–227.

Brown, R.D., Gillespie, T.J., 1986. Estimating outdoor thermal comfort using a cylindrical radiation thermometer and an energy budget model. Int. J. Biometeorol. 30 (1), 43–52.

Butte, Nancy F., et al., 2018. A youth compendium of physical activities: activity codes and metabolic intensities. Med. Sci. Sports Exerc. 50 (2), 246–256.
Campbell-Lendrum, Diarmid, Corvalán, Carlos, 2007. Climate change and developing-country cities: implications for environmental health and equity. J. Urban Health 84 (Suppl. 1), 109–117.
Castaldo, V.L., Coccia, V., Cotana, F., Pignatta, G., Pisello, A.L., Rossi, F., 2015. technique 14, 301. https://doi.org/10.1016/j.uclim.2015.05.006.
Cheng, Wenwen, Brown, Robert D., 2020. An energy budget model for estimating the thermal comfort of children. Int. J. Biometeorol. 64 (8), 1355–1366.
Chu, Dinh Toi, et al., 2019. "An update on obesity: mental consequences and psychological interventions." Diabetes and Metabolic Syndrome. Clinical Research and Reviews 13 (1), 155–160. https://doi.org/10.1016/j.dsx.2018.07.015.
Falk, Bareket, Dotan, Raffy, 2008. Children's thermoregulation during exercise in the heat - a revisit. Appl. Physiol. Nutr. Metab. 33 (2), 420–427.
Falk, Bareket, Bar-or, Oded, Calvert, Randy, Macdougall, J. Duncan, 1991. Sweat gland response to exercise in the heat among pre-, mid-, and late- pubertal boys. Official Journal of the American College of Sports Medicine 24, 313–319.
Fabiani, C., Pisello, A.L., Bou-Zeid, E., Yang, J., Cotana, F., 2019. Adaptive measures for mitigating urban heat islands: The potential of thermochromic materials to control roofing energy balance. Applied Energy 247, 155–170. https://doi.org/10.1016/j.apenergy.2019.04.020.
Haycock, George B., Schwartz, George J., Wisotsky, David H., 1978. Geometric method for measuring body surface area: a height-weight formula validated in infants, children, and adults. J. Pediatr. 93 (1), 62–66.
Hoornweg, Daniel, Sugar, Lorraine, Gómez, Claudia Lorena Trejos, 2011. Cities and greenhouse gas emissions: moving forward. Environ. Urban. 23 (1), 207–227.
Huang, Boze, et al., 2021. Outdoor thermal benchmarks and thermal safety for children: a study in China's cold region. Sci. Total Environ. 787, 147603 https://doi.org/10.1016/j.scitotenv.2021.147603.
Hugh, A., et al., 2009. Preventing Physical Activity Induced Heat Illness in School Settings, July, pp. 8–10.
Jessel, Sonal, Sawyer, Samantha, Hernández, Diana, 2019. Energy, poverty, and health in climate change: a comprehensive review of an emerging literature. Front. Public Health 7 (December).
Kim, Young Jae, Lee, Chanam, Kim, Jun Hyun, 2018. Sidewalk landscape structure and thermal conditions for child and adult pedestrians. Int. J. Environ. Res. Public Health 15 (1).
Kleerekoper, Laura, Van Esch, Marjolein, Salcedo, Tadeo Baldiri, 2012. How to make a City climate-proof, addressing the urban Heat Island effect. Resour. Conserv. Recycl. 64, 30–38. https://doi.org/10.1016/j.resconrec.2011.06.004.
Kottek, Markus, et al., 2006. World map of the Köppen-Geiger climate classification updated. Meteorol. Z. 15 (3), 259–263.
Landing, Benjamin H., Wells, Theadis R., 1969. Sweat gland anatomy in genetic diseases. J. Chronic Dis. 21 (9–10), 703–713.
Laschewski, G., Jendritzky, G., 2002. Effects of the thermal environment on human health: an investigation of. Clim. Res. 21 (1), 91–103.
Lee, Hyunjung, Holst, Jutta, Mayer, Helmut, 2013. Modification of human-biometeorologically significant radiant flux densities by shading as local method to mitigate heat stress in summer within urban street canyons. Adv. Meteorol. 2013.
Lee, Ivan, Voogt, James A., Gillespie, Terry J., 2018. Analysis and comparison of shading strategies to increase human thermal comfort in urban areas. Atmosphere 9 (3).
Mazhar, Naveed, Brown, Robert D., Kenny, Natasha, Lenzholzer, Sanda, 2015. Thermal comfort of outdoor spaces in Lahore, Pakistan: lessons for bioclimatic Urban Design in the context of global climate change. Landsc. Urban Plan. 138, 110–117. https://doi.org/10.1016/j.landurbplan.2015.02.007.
Middel, Ariane, Selover, Nancy, Hagen, Björn, Chhetri, Nalini, 2016. Impact of shade on outdoor thermal comfort—a seasonal field study in Tempe, Arizona. Int. J. Biometeorol. 60 (12), 1849–1861. https://doi.org/10.1007/s00484-016-1172-5.
Mors, Sander ter, Hensen, Jan L.M., Loomans, Marcel G.L.C., Boerstra, Atze C., 2011. Adaptive thermal comfort in primary school classrooms: creating and validating PMV-based comfort charts. Build. Environ. 46 (12), 2454–2461. https://doi.org/10.1016/j.buildenv.2011.05.025.
Nikolopoulou, Marialena, Lykoudis, Spyros, 2006. Thermal comfort in outdoor urban spaces: analysis across different European countries. Build. Environ. 41 (11), 1455–1470.
Oke, T.R., 1982. The energetic basis of the urban Heat Island. Q. J. R. Meteorol. Soc. 108 (455), 1–24.
Pénard-Morand, C., et al., 2010. Long-term exposure to close-proximity air pollution and asthma and allergies in urban children. Eur. Respir. J. 36 (1), 33–40.
Peng, Wangchongyu, et al., 2022. Surface and canopy urban Heat Islands: does urban morphology result in the spatiotemporal differences? Urban Clim. 42 (December 2021), 101136 https://doi.org/10.1016/j.uclim.2022.101136.
Ridha, Suaad, Ginestet, Stéphane, Lorente, Sylvie, 2018. Effect of the shadings pattern and greenery strategies on the outdoor thermal comfort. International Journal of Engineering and Technology 10 (2), 108–114.
Rodgers, Griffin P., Dietz, William, Lavizzo-Mourey, Risa, 2018. Research on childhood obesity: building the Foundation for a Healthier Future. Am. J. Prev. Med. 54 (3), 450–452.
Rosso, Federica, Pioppi, Benedetta, Pisello, Anna Laura, 2022. Pocket parks for human-centered urban climate change resilience: microclimate field tests and multi-domain comfort analysis through portable sensing techniques and Citizens' science. Energy and Buildings 260, 111918. https://doi.org/10.1016/j.enbuild.2022.111918.
Sánchez, Trinidad, et al., 2019. Association between air pollution and sleep disordered breathing in children. Pediatr. Pulmonol. 54 (5), 544–550.
Sathishkumar, V.E., Shin, Changsun, Cho, Yongyun, 2021. Efficient energy consumption prediction model for a data analytic-enabled industry building in a Smart City. Build. Res. Inf. 49 (1), 127–143. https://doi.org/10.1080/09613218.2020.1809983.
Schofield, W.N., 1985. Predicting basal metabolic rate, new standards and review of previous work. Human Nutrition Clinical Nutrition 39, 5–41.
Sensortec, Bosch, 2015. Bme280. In: Bosch Sensortec GmbH (BST-BME280-FL000-00), pp. 1–2.
Spagnolo, Jennifer, de Dear, Richard, 2003. A field study of thermal comfort in outdoor and semi-outdoor environments in subtropical Sydney Australia. Build. Environ. 38 (5), 721–738.
Staiger, Henning, Laschewski, Gudrun, Matzarakis, Andreas, 2019. Selection of appropriate thermal indices for applications in human biometeorological studies. Atmosphere 10 (1), 1–15.
Taleghani, Mohammad, 2018. Outdoor thermal comfort by different heat mitigation strategies- a review. Renew. Sust. Energ. Rev. 81 (June 2017), 2011–2018. https://doi.org/10.1016/j.rser.2017.06.010.
Taleghani, Mohammad, Kleerekoper, Laura, Tenpierik, Martin, Van Den Dobbelsteen, Andy, 2015. Outdoor thermal comfort within five different urban forms in the Netherlands. Build. Environ. 83, 65–78. https://doi.org/10.1016/j.buildenv.2014.03.014.
Teli, Despoina, Jentsch, Mark F., James, Patrick A.B., 2012. Naturally ventilated classrooms: an assessment of existing comfort models for predicting the thermal sensation and preference of primary school children. Energy and Buildings 53, 166–182. https://doi.org/10.1016/j.enbuild.2012.06.022.
Thorsson, Sofia, et al., 2007. Thermal comfort and outdoor activity in Japanese urban public places. Environ. Behav. 39 (5), 660–684.
Tsuzuki-Hayakawa, Kazuyo, Tochihara, Yutaka, Ohnaka, Tadakatsu, 1995. Thermoregulation during heat exposure of young children compared to their mothers. Eur. J. Appl. Physiol. Occup. Physiol. 72 (1), 12–17.
Vanos, Jennifer K., 2015. Children's health and vulnerability in outdoor microclimates: a comprehensive review. Environ. Int. 76, 1–15. https://doi.org/10.1016/j.envint.2014.11.016.
Vanos, Jennifer K., Herdt, Alexandria J., Lochbaum, Marc R., 2017. Effects of physical activity and shade on the heat balance and thermal perceptions of children in a playground microclimate. Build. Environ. 126, 119–131. https://doi.org/10.1016/j.buildenv.2017.09.026.
Watts, Nick, et al., 2019. The 2019 report of the lancet countdown on health and climate change: ensuring that the health of a child born today is not defined by a changing climate. Lancet 394 (10211), 1836–1878.
Weyrich, Tim, et al., 2006. Analysis of Human Faces Using a Measurement-Based Skin Reflectance Model. In: *ACM SIGGRAPH 2006 Papers, SIGGRAPH '06*: 1013–24.
World Maps of Köppen-Geiger Climate Classification. http://koeppen-geiger.vu-wien.ac.at/present.htm, 2023.
Zhao, Caijun, Guobin, Fu, Liu, Xiaoming, Fan, Fu., 2011. Urban planning indicators, morphology and climate indicators: a case study for a north-south transect of Beijing, China. Build. Environ. 46 (5), 1174–1183. https://doi.org/10.1016/j.buildenv.2010.12.009.